Molecular Pharmacology Fast Forward. Published on December 1, 2008 as doi:10.1124/mol.108.049031
This article has not been copyedited and formatted. The final version may differ from this version.

Title page

Differential coupling of the vasopressin V_{1b} receptor through compartmentalization within the plasma membrane

Hélène Orcel, Laura Albizu, Sanja Perkovska, Thierry Durroux, Christiane Mendre, Hervé Ansanay, Bernard Mouillac and Alain Rabié

CNRS, UMR 5203, Institut de Génomique Fonctionnelle, Montpellier, France and INSERM, U661, Montpellier, France and Université Montpellier, 1, 2, Montpellier, France (H.O., L.A., S.P., T.D., C.M.,B.M., A.R.); Cisbio bioassays, Bagnols-sur-Cèze, France (H.A.)

Molecular Pharmacology Fast Forward. Published on December 1, 2008 as DOI: 10.1124/mol.108.049031
This article has not been copyedited and formatted. The final version may differ from this version.

Running title page

Running title: **Dual signaling of the vasopressin V_{1b} receptor**

Corresponding author:

Dr Alain Rabié,

Institut de Génomique Fonctionnelle, 141 rue de la Cardonille, 34094 MONTPELLIER Cedex 5, France

Tel.: (33) 4 67 14 29 58

Fax: (33) 4 67 54 24 32

E-mail: alain.rabie@igf.cnrs.fr

Text pages (number): *30*

Tables (number): *3*

Figures (number): *6*

References (number): *44*

Abstract (words): *237*

Introduction (words): *601*

Discussion (words): *1414*

ABBREVIATIONS: AVP, arginine-vasopressin; AVT, arginine-vasotocin; BRET, bioluminescence resonance energy transfer; BSA, bovine serum albumin; Ctx, cholera toxin; d[Cha^4]AVP, [1-deamino-4-cyclohexylalanine] arginine-vasopressin; FBS, fetal bovine serum; FRET, fluorescence resonance energy transfer; GPCR, G protein-coupled receptor; HA-tag, hemagglutinin tag; 6xHis-tag, hexahistidine tag; HTRF®, homogeneous time-resolved fluorescence; IP, inositol phosphates; MßCD, methyl-ß-cyclodextrin; OT, oxytocin; Ptx, pertussis toxin.

Molecular Pharmacology Fast Forward. Published on December 1, 2008 as DOI: 10.1124/mol.108.049031
This article has not been copyedited and formatted. The final version may differ from this version.

ABSTRACT

We show here that the rat vasopressin V_{1b} receptor simultaneously activates both the $G_{q/11}$-IP and G_s-cAMP pathways when transiently expressed in CHO, HEK-293, and COS-7 cells and stimulated with arginine-vasopressin. Higher concentrations of the hormone, however, were needed to trigger the cAMP pathway. The non-mammalian analog arginine-vasotocin and the selective V_{1b} agonist d[Cha^4]vasopressin also activated the cAMP and IP pathways, although d[Cha^4]vasopressin elicited the two responses with equivalent potencies. We determined that the V_{1b} receptor is present as homodimers at the plasma membrane. Treatment of V_{1b}-transfected HEK-293 cells with methyl-ß-cyclodextrin, a drug known to dissociate cholesterol-rich domains of the plasma membrane, shifted the EC_{50} of the vasopressin-induced cAMP accumulation to lower concentrations and, remarkably, increased the hormone efficacy related to the activation of this second messenger system. In parallel, the vasopressin-mediated activation of the IP pathway was slightly reduced without modification of its EC_{50}. These results suggest that, as with many other G protein-coupled receptors, when transfected in heterologous cell systems, the V_{1b} receptor forms dimers that signal differentially through the $G_{q/11}$ and G_s proteins depending on the nature of the ligand as well as on its localization within specialized compartments of the plasma membrane. The present study thus illustrates how signal transduction associated with the activation of a G protein-coupled receptor can be versatile and highly dependent on both the cell context and the chemical nature of the extracellular signaling messenger.

Molecular Pharmacology Fast Forward. Published on December 1, 2008 as DOI: 10.1124/mol.108.049031
This article has not been copyedited and formatted. The final version may differ from this version.

Introduction

Increasing evidence indicates that G protein-coupled receptor (GPCR) signaling can achieve specificity in different ways. The previously accepted linear signaling concept has evolved into a network concept that allows for more possibilities with respect to the fine tuning of various pathways. The differential activation or inactivation of G protein-dependent or -independent signaling pathways can occur at various levels (Hermans, 2003; Michel and Alewijnse, 2007; Swaminath et al., 2005). First, receptors can adopt different active and inactive conformational states depending on the ligands they bind, resulting in multiplicity of coupling (Kenakin 2003). Second, GPCRs have the propensity to homo- or hetero-dimerize, leading to variations in their pharmacological properties (Terrillon and Bouvier, 2004; Park and Palczewski, 2005; Milligan, 2006). Finally, the receptor environment, in particular the localization of receptors within specialized microdomains of the plasma membrane such as rafts or caveolae, can profoundly modify their coupling properties and cause them to switch from one signaling pathway to another (Gimpl and Fahrenholz, 2000; Guzzi et al., 2002; Rimoldi et al., 2003). All of these aspects can contribute to the interaction of GPCRs with different protein complexes and can thus explain cell-dependent signaling variability and how signaling can be channeled into specific routes in particular cells (Schulte and Levy, 2007). Accordingly, such aspects must be taken into consideration to have a complete understanding of a given receptor's cellular lifespan and to develop new selective therapeutic compounds.

We have focused our work on the arginine-vasopressin (AVP) V_{1b} receptor. This GPCR, which is expressed in numerous peripheral tissues (e.g. pituitary gland and adrenal gland) and various areas of the nervous system (Lolait et al., 1995; Hurbin et al., 1998; Vaccari et al., 1998; Hernando et al., 2001; Young et al., 2006), is involved in stress behavior and represents an interesting therapeutic target for psychiatric disorders such as anxiety or depression (Serradeil-Le Gal et al., 2002). In this context, studying its functional activation properties is of importance.

Molecular Pharmacology Fast Forward. Published on December 1, 2008 as DOI: 10.1124/mol.108.049031
This article has not been copyedited and formatted. The final version may differ from this version.

Previous studies have suggested that the V_{1b} receptor can exhibit differential coupling, as has been shown for other members of the AVP/oxytocin (OT) receptor family (V_{1a}, V_2, and OT receptors). Indeed, other members of the family signal either through pathways involving different G proteins (Abel et al., 2000; Zhou et al., 2007) or even through G protein-independent pathways (Charest et al., 2007; Rimoldi et al., 2003). With respect to the V_{1b} receptor, previous work has shown that it activates the IP pathway via coupling to the $G_{q/11}$ protein (Jard et al., 1986). Signaling through the cAMP pathway has been reported in stably transfected CHO cells, although it was interpreted as nonspecific coupling to G_s due to overexpression (Thibonnier et al., 1997). In addition, an atypical response of the V_{1a} and/or V_{1b} receptors towards the cAMP pathway was suspected in the vasopressinergic magnocellular neurons of the supraoptic nucleus (Hurbin et al., 1998). Specifically, AVP triggered an adenylyl cyclase-mediated intracellular response in these cells through a mechanism that is not yet understood since the G_s-coupled V_2 receptor is not expressed (Gouzènes et al., 1999; Hurbin et al., 1998; Sabatier et al., 1998).

To investigate the potential multiple coupling properties of the rat V_{1b} receptor, we asked whether: (i) this receptor can activate both the IP and cAMP signaling pathways at low levels of expression and in different cell systems; (ii) a link could be established between the nature of the ligand on the one hand and the signaling pathway activated or intensity of the response on the other hand; (iii) the receptor can form dimers at the cell surface; and (iv) the response depends on the localization of the receptor within specialized plasma membrane microdomains.

Materials and Methods

cDNA constructs. Rat AVP V_{1b} receptor cDNA was obtained by RT-PCR. Total RNA was extracted from carefully dissected rat pituitary glands using the RNeasy kit (Qiagen, Courtaboeuf, France). Forward (5'-CACCTCTAAACCTTTCTCTCTCATTCC-3') and reverse (5'-GGATTGAGTGCTCTGATTTCCAAC-3') V_{1b}-specific primers were synthesized by Sigma Genosys

Molecular Pharmacology Fast Forward. Published on December 1, 2008 as DOI: 10.1124/mol.108.049031
This article has not been copyedited and formatted. The final version may differ from this version.

(St-Quentin-Fallavier, France). Reverse transcription was performed on RNA extracts previously digested with deoxyribonuclease I (Invitrogen, Cergy-Pontoise, France), using SuperScript II reverse transcriptase (Invitrogen), RNAsin (Promega Corp, Charbonnières, France) as an RNase inhibitor, and the reverse primer. DNA amplification was performed using a PTC-150/16 thermal controller (MJ Research, Inc., Watertown, MA), Platinum P*fx* DNA polymerase (Invitrogen), the reverse primer previously used for reverse transcription, and the forward primer. N-terminal tags (hexahistidine, 6xHis-tag; or hemagglutinin, HA-tag) were introduced in a second PCR step using specific primers designed to also add two restriction sites (5' Bam HI and 3' Xho I) to control the direction of fragment insertion. The PCR products were electrophoresed on a 1% agarose gel in TAE buffer (40 mM Tris-acetate, 1 mM EDTA, pH 8) and purified using GenElute columns (Sigma). Double digestion of the DNA ends with Bam HI and Xho I was performed, and the main fragment containing the V_{1b} coding sequence was purified and ligated with T4 DNA Ligase (Roche, Meylan, France) into pcDNA3.1(+) vector (Invitrogen) that had been digested with the same restriction enzymes and dephosphorylated using alkaline phosphatase (Roche). The sequence was verified by sequencing of both strands (Genome Express, Meylan, France). Using the same procedure, rat AVP V_{1a} receptor cDNA was prepared using specific forward (5'-CCTCAGGACCAGACAGAAGTAGG-3') and reverse (5'-CCACATAAACACATCTGCTCTTACG-3') primers and RNA extracted from liver. The N-terminal 6xHis-tag and restriction sites (5' Bam HI and 3' Xho I) were then added by PCR and the sequence inserted by T4 ligation into the pcDNA3.1(+) vector as indicated above.

Cell culture and transfection. Cell lines were obtained from the American Type Culture Collection (Rockville, MD). Cell culture media, fetal bovine serum (FBS), and additives were provided by Invitrogen (Cergy-Pontoise, France).

CHO, HEK-293, and COS-7 cells were grown in DMEM supplemented with 10% FBS, 100 U/ml penicillin/streptomycin, and 2 mM L-glutamine, at 37 °C in a humidified atmosphere of 95% air and 5% CO_2. For the CHO cell line, non-essential amino acids (Invitrogen) were also added to the media.

Transient transfection of the cell lines was performed using electroporation in a 300 µl volume with a total of 10 µg DNA (V_{1b} plasmid up to 1 µg plus pcDNA3.1 as carrier DNA to reach 10 µg)

Molecular Pharmacology Fast Forward. Published on December 1, 2008 as DOI: 10.1124/mol.108.049031
This article has not been copyedited and formatted. The final version may differ from this version.

containing 10^7 cells in electroporation buffer (50 mM K_2HPO_4, 20 mM CH_3COOK, 20 mM KOH, 26 mM $MgSO_4$, pH 7.4). After electroporation (260-280 V, 1 mF, GeneZapper 450/2500, IBI, New Haven, CT), cells were suspended in complete medium and seeded into 96-well culture plates at a density of 100,000 (ELISA and cAMP pathway test) or 80,000 (IP pathway test) cells per well. 96-well culture plates were first coated with polyornithine diluted in PBS, incubated at 37 °C for one hour, and then rinsed with PBS before seeding. 24 hours post-transfection, receptor expression was measured by radioligand binding assay or ELISA and the experiments on receptor dimerization and signaling pathways performed. To improve the expression of the transfected receptors, CHO and HEK-293 cells were incubated overnight with 3 mM sodium butyrate before the experiments. This treatment was not necessary with the COS-7 cells.

ELISA. To measure the expression of the transfected receptors, cells were fixed with 4% paraformaldehyde in PBS for 5 min and rinsed three times with PBS. A blocking step of 30 min with PBS + 1% decomplemented FBS was performed before incubation with the primary antibodies (0.5 µg/ml) for 30 min. The cells were then rinsed four times for 5 min in PBS + 1% FBS and incubated for 30 min with an anti-mouse antibody conjugated with horseradish peroxidase (1/1000) (Amersham, Orsay, France). The cells were rinsed three times with PBS + 1% FBS and three times with PBS. Afterwards, 60 µl PBS and 20 µl Supersignal ELISA Femto (Perbio-Pierce, Brebières, France) were added to the wells. The luminescence was read using a Wallac Victor^2 (Perkin Elmer, Courtaboeuf, France).

Second messenger (IP_1 and cAMP) accumulation. Activation/inhibition of the IP and cAMP pathways by AVP receptor agonists or antagonists, respectively, was determined using the IP-One and cAMP dynamic kits (Cisbio bioassays, Bagnols-sur-Cèze, France). Briefly, after transfection, 80,000 (IP pathway test) or 100,000 (cAMP pathway test) cells were distributed in 100 µl of complete medium into a 96-well assay plate (Greiner Bio-One, Courtaboeuf, France). Twenty-four hours later, the medium was removed and replaced with 50 µl incubation medium containing the agonist and/or antagonist at the appropriate concentrations. The IP-One test is based on the accumulation of IP_1, a downstream metabolite of the IP pathway that is produced by phospholipase C activated by the $G_{q/11}$ protein; IP_1 is stable in the presence of LiCl. The cAMP dynamic test is based on the accumulation of

Molecular Pharmacology Fast Forward. Published on December 1, 2008 as DOI: 10.1124/mol.108.049031
This article has not been copyedited and formatted. The final version may differ from this version.

cAMP produced by adenylyl cyclase activated by G_s protein; a phosphodiesterase inhibitor, Ro-20-1724 (Calbiochem, Darmstadt, Germany), prevents cAMP degradation. The homogeneous time-resolved fluorescence-fluorescence resonance energy transfer (HTRF®-FRET) assay was performed as described (Maurel et al., 2004). This assay involves the transfer of energy from a europium cryptate pyridine-bipyridine donor fluorophore to a d2 acceptor fluorophore. The assay is an immunoassay that measures competition between native IP_1 or cAMP produced by the cells and IP_1 or cAMP labeled with the d2 acceptor, as revealed by a monoclonal antibody against IP_1 or cAMP labeled with europium cryptate pyridine-bipyridine. 25 µl of antibody and 25 µl of competitor diluted in lysis buffer provided in the kits were added to the wells after 30 min incubation at 37 °C with the agonist. As a negative control, some wells only received the donor fluorophore-labeled antibody. After 1 h incubation at room temperature, fluorescence emissions were measured at both 620 nm and 665 nm on a RubyStar fluorometer (BMG Labtechnologies, Offenburg, Germany) equipped with a nitrogen laser as the excitation source (337 nm). A 400-µs reading was recorded after a 50-µs delay to eliminate the short-lived fluorescence background from the acceptor fluorophore-labeled antibody. The fluorescence intensities measured at 620 nm and 665 nm correspond to the total europium cryptate emission and to the FRET signal, respectively. The specific FRET signal was calculated using the following equation: $\Delta F\% = 100 \times (R_{pos} - R_{neg})/(R_{neg})$, with R_{pos} being the fluorescence ratio (665 nm/620 nm) calculated in wells incubated with both donor- and acceptor-labeled antibodies, and R_{neg} being the same ratio for the negative control incubated only with the donor fluorophore-labeled antibody. The FRET signal ($\Delta F\%$), which is inversely proportional to the concentration of IP_1 or cAMP in the cells, was then transformed into IP_1 or cAMP accumulation using a calibration curve prepared on the same plate. It is worth noting that all comparisons of agonist or antagonist effects were done on the same day, on the same culture and plate, and were made against the AVP effect. The experiments were repeated at least three times on different cultures. Normalization was performed as indicated in the figure legends, either as a percentage of the maximal value or as a percentage of the maximal value for AVP when comparisons were necessary. Values corresponding to the low basal activities, determined in unstimulated cells, were first subtracted. Activation/inhibition curves were plotted to the log of agonist

Molecular Pharmacology Fast Forward. Published on December 1, 2008 as DOI: 10.1124/mol.108.049031
This article has not been copyedited and formatted. The final version may differ from this version.

or antagonist concentrations and fitted to the Hill equation to extract the EC_{50}, Hill coefficient, and minimal/maximal values.

Overnight pre-incubation of cells with either cholera toxin (Ctx) (20 µg/ml culture medium) or pertussis toxin (Ptx) (100 ng/ml culture medium) was used to test the involvement of the G_s and G_i proteins in V_{1b} receptor cAMP signaling in response to AVP. When used to directly activate adenylyl cyclase, forskolin was added for 30 min at 50 µM.

The inhibitory effect of the specific non-peptidic V_{1b} antagonist, SSR149415 (Serradeil-Le Gal et al., 2002), on IP_1 and cAMP accumulations induced by AVP was studied according to Arunlakshana and Schild (1959). Pre-incubation for 10 min with the antagonist was followed by 30 min incubation with the antagonist and AVP. Concentrations of AVP greater than 1 µM were not tested here and more generally in this study since, in our experimental conditions, they often led to non specific effects. Therefore, we cannot formally insure that the inhibition by SSR149415 is stricly competitive.

Incubation of cells with methyl-ß-cyclodextrin (MßCD) (Sigma) was used to study how removing cholesterol from the plasma membrane affects V_{1b} receptor signaling. Pre-incubation at 37 °C for 10 min with 10 mM MßCD in incubation medium was followed by 30 min incubation with 10 mM MßCD plus the agonist serial dilutions. IP_1 and cAMP accumulations were then measured as described above.

RT-PCR. We performed RT-PCR on RNA extracts of COS-7 cells (which are derived from *Chlorocebus aethiops*, African green monkey) to detect the suspected expression of endogenous AVP V_2 receptor mRNA. Forward (5'-GCTAGTGATTGTGGTCGTCTATGTGC-3') and reverse (5'-CACGCTGCTGCTGAAAGATGC-3') primers were designed based on the human V_2 receptor sequence to amplify a 178 bp band from the three primate V_2 receptor sequences available to date (*Homo sapiens, Pan troglodytes, Macaca mulatta*). An intron lies between the two primer sites to ensure the rejection of undesired amplification of any residual genomic DNA. RT-PCR was performed as described above.

Radioligand binding assays to intact cells. The first binding assay was carried out with [^{3}H]AVP to determine the amount of functional receptor present at the plasma membrane of

Molecular Pharmacology Fast Forward. Published on December 1, 2008 as DOI: 10.1124/mol.108.049031
This article has not been copyedited and formatted. The final version may differ from this version.

transfected CHO and HEK-293 cells. After electroporation, cells were seeded in 24-well plates at a density of 400,000 cells/well. Binding assays were performed after 24 h. Cells were washed twice in ice-cold Tris/Krebs buffer (20 mM Tris-HCl pH 7.4, 118 mM NaCl, 5.6 mM glucose, 1.2 mM KH_2PO_4, 1.2 mM $MgSO_4$, 4.7 mM KCl, 1.8 mM $CaCl_2$) with 0.1% bovine serum albumin (BSA), after which each well received 0.2 ml of ice-cold Tris/Krebs buffer + 0.1% BSA + 5 mM phenylalanine and the appropriate dilution of [^{3}H]AVP (0.25 to 8 nM). Plates were incubated for 4 h in the cold room before removal of the binding mixture by aspiration. After quickly rinsing three times with ice-cold Krebs buffer + 0.1% BSA, 0.3 ml of 0.1 N NaOH was added to each well to lyse the cells and extract the radioactivity. The fluid from the wells was then neutralized, transferred to scintillation vials, and counted on a ß-counter (Tri-Carb 2100TR, Perkin-Elmer, Waltham, MA). Non-specific binding was determined under the same conditions in the presence of 10 µM unlabeled AVP. Protein levels were determined using the BCA protein assay (Pierce Biotechnology, Rockford, IL). The experiment was repeated three times on different cultures. Maximal binding capacity and dissociation constants were determined from the Scatchard transformation of the saturation binding curves.

The second binding assay was done to determine, through a competition experiment, the inhibitory dissociation constant (K_i) of arginine-vasotocin (AVT) for the rat AVP V_{1b} receptor. Cells were incubated with a fixed concentration of [^{3}H]AVP (2 nM) that was displaced using increasing concentrations of AVT (10^{-12} to 10^{-6} M). The experiment was repeated three times on different cultures. Displacement curves were fitted to determine the IC_{50} values, which were then converted to K_i using the Cheng-Prusoff equation: $K_i=IC_{50}/(1+L/K_d)$, where L represents the concentration of [^{3}H]AVP and K_d the dissociation constant of AVP for the rat V_{1b} receptor in intact CHO cells determined as indicated above.

Receptor dimerization at the plasma membrane. Dimerization was measured using an HTRF®-FRET assay. Monoclonal anti-6xHis and/or anti-HA antibodies labeled with a europium cryptate pyridine-bipyridine donor fluorophore or a d2 acceptor fluorophore (Cisbio bioassays) were used. After transfection, 100,000 COS-7 cells/well were transferred to a black 96-well assay plate (Greiner) in 100 µl complete medium. Twenty-four hours later, COS-7 cells expressing the 6xHis- or

Molecular Pharmacology Fast Forward. Published on December 1, 2008 as DOI: 10.1124/mol.108.049031
This article has not been copyedited and formatted. The final version may differ from this version.

HA-tagged rat receptors were incubated at 4 °C in 100 µl Tris/Krebs buffer (20 mM Tris-HCl pH 7.4, 118 mM NaCl, 5.6 mM glucose, 1.2 mM KH_2PO_4, 1.2 mM $MgSO_4$, 4.7 mM KCl, 1.8 mM $CaCl_2$) supplemented with 0.1% BSA and containing 1 nM europium cryptate pyridine-bipyridine- and 1 nM d2-labeled antibodies. To obtain the negative control value, some COS-7 cells were incubated with the donor fluorophore-labeled antibody only. Fluorescence intensities were measured at 620 nm and 665 nm and the FRET signal (ΔF%), reflecting dimerization, calculated as described above. The experiments were repeated at least three times on different cultures.

Statistical analysis. Statistical significance of the differences between experimental groups was determined by one-way or two-way analysis of variance followed by a post-hoc Duncan's multiple range test to make pairwise comparisons between means. Student *t* test was also used.

Results

The rat V_{1b} receptor signals through both the IP and cAMP pathways. AVP stimulation of CHO, HEK-293 and COS-7 cells transfected with 1 µg of rat V_{1b} receptor-encoding plasmid led to the activation of both the IP and cAMP pathways measured as accumulation of IP_1 and cAMP, respectively (Fig. 1). The responses were specific for V_{1b} receptor expression, since mock CHO and HEK-293 cells (transfected with an empty pcDNA3 vector) did not exhibit any response to AVP (Fig. 1A,B). Similar patterns of IP_1 and cAMP accumulation were observed with transiently transfected COS-7 cells (Fig. 1C), despite the presence of endogenous V_2 receptor which was responsible for about 20% of the cAMP production as demonstrated in mock cells. The presence of this endogenous receptor was confirmed by RT-PCR performed using primers specific for primate V_2 receptor sequences, revealing the endogenous V_2 receptor mRNA in COS-7 cell extracts (data not shown).

The dual coupling was not due to overexpression of V_{1b} receptors (448,000 receptors/cell, compared to 36,000 receptors/cell in corticotrophs of the adenohypophysis; Gaillard et al., 1984) since it was still observed when lowering V_{1b} receptors expression (31,410 receptors/cell) to a similar level than the physiological one (Supplemental Fig. 1).

Molecular Pharmacology Fast Forward. Published on December 1, 2008 as DOI: 10.1124/mol.108.049031
This article has not been copyedited and formatted. The final version may differ from this version.

Differential activation of IP and cAMP pathways following AVP stimulation. Although AVP stimulated both the IP and cAMP signaling pathways, it is worth noting that in the three cell lines tested AVP stimulated the accumulation of IP_1 at lower concentrations than that of cAMP (Fig. 1A-C). Specifically, as shown in Table 1, the EC_{50} values for the IP accumulation, which were very close to the K_d values, were consistently 3-5 times lower than those obtained for the cAMP accumulation. This has been observed whatever the V_{1b} receptor expression level. Moreover, in both CHO and HEK-293 cells, where no endogenous V_2 receptor disturbs the response, the Hill coefficients of the activation curves were lower for the IP pathway than for the cAMP pathway. Reliable similar analyses of COS-7 cell parameters were not possible because of the presence of endogeneous V_2 receptor.

To confirm that the cAMP pathway is directly stimulated by the V_{1b} receptor, we examined the involvement of G_s. Specifically, we treated transfected CHO cells overnight with cholera toxin (Ctx), to induce direct and sustained stimulation of G_s. As expected, under these conditions cAMP accumulation was much higher, but AVP had no additive effect (Fig. 2A). This absence of effect of AVP under Ctx treatment was not due to saturation of adenylyl cyclase activity, since simultaneous treatment of the cells with Ctx and forskolin further increased cAMP accumulation (by 53.0 $\pm$ 4.2 times, data not shown). It can thus be inferred from these two observations that the stimulation of the V_{1b} receptor by AVP requires the G_s protein to activate the cAMP pathway. By contrast, the V_{1b} receptor did not stimulate the G_i or G_o protein, since an overnight treatment with pertussis toxin (Ptx) did not affect the AVP-induced cAMP accumulation (Fig. 2B). As a positive control, such a treatment inhibited the serotonin-induced response of the G_i-coupled human $5HT_{1a}$ receptor (Supplemental Fig. 2).

AVP analogs activate the IP and cAMP pathways in different manners. To address whether the two signaling pathways exhibit different pharmacological properties, we examined the effects on both pathways of one specific non-peptidic V_{1b} antagonist, SSR149415 (Serradeil-Le Gal et

Molecular Pharmacology Fast Forward. Published on December 1, 2008 as DOI: 10.1124/mol.108.049031
This article has not been copyedited and formatted. The final version may differ from this version.

al., 2002), and two peptidic agonists of AVP, arginine-vasotocin (AVT), the non-mammalian vertebrate ortholog of AVP, and d[Cha^4]AVP, a specific V_{1b} receptor agonist (Guillon et al., 2006).

IP_1 and cAMP accumulations in V_{1b}-transfected CHO cells stimulated with increasing AVP concentrations was studied without or with increasing amounts of SSR149415. The resulting Arunlakshana-Schild plots showed that both the IP and cAMP pathways were turned off (Fig. 3). Interestingly, the antagonist affected the cAMP accumulation at lower concentrations (pA_2 = 9.99, ie K_{inact} = 0.10 nM) than the IP_1 accumulation (pA_2 = 9.14, ie K_{inact} = 0.72 nM) (Fig. 3; Table 2).

Although the two agonists tested, AVT and d[Cha^4]AVP, stimulated both pathways, the curves differed from those obtained with AVP (Fig. 4). As with AVP, AVT activated both the IP and cAMP pathways, but did it with lower EC_{50} values than AVP (Fig. 4A; Table 2). Again, it is worth noting that the EC_{50} of the IP_1 accumulation curve was lower than that of the cAMP one and was very close to the affinity of AVT for the V_{1b} receptor measured in binding experiments (Table 2). The stimulation of IP signaling by AVT was similar to that by AVP with respect to the slopes of the curves (Table 2) and the maximal stimulation values (Table 2). By contrast, cAMP stimulation by AVT differed from that by AVP in that it had a steeper slope (Fig. 4A; Table 2) and showed a 36% higher level of maximal stimulation (Table 2). AVT is thus a more potent and more efficacious agonist than AVP on the cAMP pathway.

d[Cha^4]AVP also activated both the IP and cAMP pathways, but did not show any differences in the activation of the two pathways, and the dose-response curves for IP_1 and cAMP accumulation were superimposed (Fig. 4B**)**. In both cases, high concentrations of d[Cha^4]AVP were necessary to elicit the response (Fig. 4B; Table 2), even though the affinity of this compound for the rat V_{1b} receptor is known to be 1.4 nM in CHO cells (Guillon et al., 2006). Both curves exhibited a slope factor of around 1 and lower maximal stimulation levels than those observed with AVP (- 18% and - 59% for the IP and cAMP pathways, respectively; Table 2). Therefore, d[Cha^4]AVP was shown to be a partial agonist of the IP and cAMP pathways when compared to AVP or AVT.

Dimers of rat V_{1b} receptors detected at the plasma membrane. Slope factors greater than 1 (1.67 for AVT on cAMP accumulation) or less than 1 (AVP and AVT on IP_1 accumulation) were

Molecular Pharmacology Fast Forward. Published on December 1, 2008 as DOI: 10.1124/mol.108.049031
This article has not been copyedited and formatted. The final version may differ from this version.

observed. Among other hypotheses such as binding site heterogeneity of the ligand for the receptor and/or of the ligand-receptor complexes for G proteins, these slope factors different from 1 strongly suggested the existence of crosstalk between receptors. Since crosstalk between receptors has been related to dimerization in various reports (Terrillon and Bouvier, 2004; Park and Palczewski, 2005; Milligan, 2006; Urban et al., 2007), we tested whether the rat V_{1b} receptor is able to dimerize at the plasma membrane. DNA encoding the rat V_{1b} receptor, tagged with the 6xHis epitope at the extracellular N-terminus, was transiently transfected into COS-7 cells and HTRF® technology used to quantify dimers at the cell surface. As a positive control for dimerization, COS-7 cells from the same culture were transfected with a rat V_{1a} receptor that had similarly been tagged with the 6xHis epitope. In both cases, a FRET signal was observed for the V_{1a} receptor (ΔF=236%) and the V_{1b} receptor (ΔF=128%) (Fig. 5A) when expressed at similar levels (Fig. 5B). The specificity of the FRET signal was demonstrated by (i) the absence of signal in mock cells; (ii) the relationship between the amount of V_{1b} receptor expressed at the membrane and the FRET signal: SSR149415 (1 µM, overnight), by acting as a pharmacochaperone on the receptor thus facilitating its targeting to the cell membrane (Robert et al., 2005), increased membrane V_{1b} receptor by 61% (measured by ELISA, Fig. 5B and 5D) and the FRET signal by 57% (Fig. 5A and 5C); and (iii) the weak FRET signal observed (ΔF=16%) between an HA-tagged human $GABA_{B2}$ receptor (a member of the GPCR C family) and the 6xHis-tagged V_{1b} receptor in comparison to the signal obtained with the HA-V_{1b} and 6xHis-V_{1b} receptors (71%) (Fig. 5C). The weak signal was not due to low HA-$GABA_{B2}$ receptor expression, as the HA-$GABA_{B2}$ and HA-V_{1b} receptors were expressed at similar levels (Fig. 5D). Instead, it probably resulted from the simple promiscuity of the receptors.

Lowering plasma membrane cholesterol modifies V_{1b} receptor signaling. The OT receptor has been shown to activate both the $G_{q/11}$ and G_i pathways, and these dual properties are dependent on the localization of the receptor to specialized domains of the plasma membrane (Gimpl and Fahrenholz, 2000; Guzzi et al., 2002; Rimoldi et al., 2003). We thus decided to investigate whether the activation levels of the two signaling pathways triggered by stimulating the V_{1b} receptor would be similarly affected by alterations in receptor localization within different membrane compartments.

Molecular Pharmacology Fast Forward. Published on December 1, 2008 as DOI: 10.1124/mol.108.049031
This article has not been copyedited and formatted. The final version may differ from this version.

Since we had observed that AVP-induced IP_1 accumulation was quite similar in the CHO and HEK-293 cell lines, while AVP-induced cAMP accumulation differed strongly between the two cell types, we compared the effects of methyl-ß-cyclodextrin (MßCD), a compound known to rapidly remove more than half of the cholesterol from the plasma membrane (Kilsdonk et al., 1995), on these two cell lines.

CHO cells expressing the rat V_{1b} receptor were incubated with 10 mM MßCD. Under these conditions, the maximal AVP-induced IP_1 accumulation was significantly reduced (-30% at maximal effect), while the maximal cAMP accumulation was increased (+ 10% at maximal effect) (data not shown).

The experiments were then repeated in HEK-293 cells transfected with the V_{1b} receptor, in which only a low level of cAMP accumulation by AVP was initially observed (Table 1). When these cells were stimulated with AVP in the presence of 10 mM MßCD, IP_1 accumulation fell by 32% at maximal effect, similar to what was observed in CHO cells (Fig. 6A; Table 3). The cAMP accumulation, in contrast, showed a much higher level of activation (+234% at saturation) than it did in the absence of MßCD (Fig. 6B; Table 3). The MßCD treatment of HEK-293 cells did not change significantly the EC_{50} of the AVP-induced IP_1 accumulation (Table 3). Interestingly, the EC_{50} of the AVP-induced cAMP accumulation shifted significantly from 32.7 to 13.1 nM following MßCD treatment. The same effects on IP_1 (-31%) and cAMP (+265%) accumulations were obtained when V_{1b} receptor-transfected HEK-293 cells were stimulated with AVT instead of AVP (Fig. 6C,D; Table 3). When d[Cha^4]AVP was used to stimulate the cells, cAMP accumulation was also highly increased by MßCD treatment; as in CHO cells, activation of both pathways were observed at higher similar concentrations (Fig. 6E,F; Table 3). Together, these results clearly indicated that compartmentalization of the V_{1b} receptor in cholesterol-rich specialized domains modulates its G protein-dependent signalization.

Finally, to investigate the possibility that treatment of the cells with MßCD directly affected adenylyl cyclase activity, wild-type HEK-293 cells were stimulated with forskolin with or without treatment with MßCD. MßCD did not change the level of cAMP accumulation (Fig. 6G).

Molecular Pharmacology Fast Forward. Published on December 1, 2008 as DOI: 10.1124/mol.108.049031
This article has not been copyedited and formatted. The final version may differ from this version.

Discussion

We observed dual signaling activity for the V_{1b} receptor: it activated both the IP pathway, as expected (Jard et al., 1986), and the cAMP pathway through coupling to the G_s protein; coupling to G_i, in contrast, was not observed. These results were not cell-line dependent as they were obtained in the three different cell lines tested. Moreover, at variance with previously reported results (Thibonnier et al., 1997), we observed that the dual signaling of the V_{1b} receptor is not restricted to cells in which the receptor is overexpressed (> 25 pmoles/mg protein), but is also observable at receptor densities in the same range as those observed in native tissues. This dual signaling was observed with various agonists, albeit with some notable differences in the activation curves. For example, while the EC_{50} values for AVP or AVT activation of the IP pathway were very close to their binding affinities, for cAMP pathway activation the EC_{50} values were 3-5 times higher. By contrast, the EC_{50} values of d[Cha^4]AVP for the IP and cAMP pathways were consistently higher than the affinity constants. Dual signaling has been previously observed for many GPCRs and in some cases, such as the corticotropin-releasing hormone receptor or the luteinizing hormone receptor, coupling to even three G proteins has been described (Hermans, 2003). In most cases, and as observed here also, the coupling occurs at different concentrations (Ashkenazi et al., 1987). In rare cases, like here with d[Cha^4]AVP, activation of the two pathways occurs at the same ligand concentration (Cussac et al., 2002). Regarding the AVP/OT receptor family, dual G protein coupling has been reported for the V_{1a} (Abel et al., 2000) and OT receptors (Strakova and Soloff, 1997), both of which couple to $G_{q/11}$ and G_i. In addition, the V_2 receptor possibly activates G_s and $G_{q/11}$ (Liu and Wess, 1996).

Although the concomitant activation of different signaling pathways has been well established, the molecular mechanisms underlying differential coupling remain unclear. A few hypotheses have been formulated to explain this phenomenon. Dual signaling and a shift between two activation curves may be explained by a difference in the affinity of the ligand-receptor complex for each G protein, or by a difference in the relative concentrations of the G proteins (Kenakin, 2003). In addition, crosstalk

Molecular Pharmacology Fast Forward. Published on December 1, 2008 as DOI: 10.1124/mol.108.049031
This article has not been copyedited and formatted. The final version may differ from this version.

between ligands, receptors, and G proteins can influence the conformations of the different partners and lead to significant differences in receptor signaling (Kenakin, 2003).

The first and probably simplest hypothesis is that the affinities of the receptor-G protein complex for the ligand are dependent on the nature of the G protein. For example, stimulation of the IP pathway by AVP and AVT could result from the binding of the ligand to the high affinity binding sites, whereas the cAMP pathway could be activated by the binding of the ligand to the low affinity binding sites. However, this hypothesis is not completely in accordance with different data: (i) the curves of IP_1 accumulation exhibit slope factors of around 0.7-0.8, indicating either negative cooperative binding or the coexistence of independent high- and low-affinity binding sites that both couple to the IP signaling pathway; (ii) the d[Cha^4]AVP-induced accumulation of both IP_1 and cAMP is shifted to the right of the binding curve, suggesting that the high affinity binding sites are devoid of any activity and that low affinity binding sites are involved in both coupling pathways; (iii) the AVT-induced cAMP pathway activation curves are steep, indicating a positive cooperative effect.

Because positive and negative cooperative effects have been related to receptor dimerization (Durroux, 2005; Springael et al., 2006; Urizar et al., 2005), we investigated the ability of rat V_{1b} to undergo oligomerization. The AVP V_{1a} and V_2 receptors, as well as the OT receptor, have previously been shown to homo- and heterodimerize (Terrillon et al., 2003). Using the HTRF® methodology and conjugated antibodies against extracellular epitopes, we have now been able to detect homodimers of V_{1b} receptors at the plasma membrane of transfected cells. As saturation and homologous competition experiments performed on the human V_{1b} receptor using radioligands have clearly demonstrated negative cooperative binding (Albizu et al., 2006), the activation of the two signaling pathways could be related to ligand-receptor stoichiometry. Moreover, as with other GPCRs, changes in V_{1b} receptor conformation upon agonist binding may differ considerably with respect to the ligand structure, the cooperativity between the two protomers in the dimer, their affinities for different G proteins, and/or their abilities to activate bound G proteins (Urban et al., 2007; Michel and Alewijnse, 2007). In accordance with the receptor dimerization hypothesis, the IP pathway could be activated by the binding of either one or two AVP molecules to a single receptor dimer. Because of the negative cooperative binding, the activation curve would thus exhibit a slope of less than 1. By contrast, cAMP

Molecular Pharmacology Fast Forward. Published on December 1, 2008 as DOI: 10.1124/mol.108.049031
This article has not been copyedited and formatted. The final version may differ from this version.

production could only be turned on upon the binding of two ligands to a dimer. Because of the negative cooperative binding, the cAMP activation curve would be observed only during the saturation of the low affinity binding sites and would thus exhibit a slope factor of around 1; it would therefore be shifted to the right of the IP activation curve. Contrary to AVP and AVT, two d[Cha^4]AVP molecules would need to bind to the receptor to induce an active receptor conformation, whatever the signaling pathway considered. Consistent with these hypotheses, the SSR149415 antagonist shuts down the cAMP pathway as soon as one AVP ligand is displaced, but does not inactivate the IP pathway until both ligands are removed.

GPCR signaling has been shown to be related to the compartmentalization of receptors or G proteins within specialized microdomains of the plasma membrane. For example, the OT receptor is able to signal through $G_{q/11}$ or G_i depending on its localization within or outside of cholesterol-rich microdomains of the cell surface (Guzzi et al., 2002; Rimoldi et al., 2003). To address whether the interactions between V_{1b} receptors and G proteins are random interactions or whether they are related to compartmentalization, we investigated the effects of MßCD, a compound that rapidly removes more than half of the cholesterol content of the plasma membrane and disrupts rafts and caveolae (Kilsdonk et al., 1995). Previous work has shown that MßCD treatment does not prevent cAMP signaling (Miura et al., 2001), and indeed we found that it had no effect on forskolin-induced cAMP production. However, it did lower the maximal IP_1 accumulation and increased the maximal cAMP accumulation. Using AVT as the stimulating ligand in HEK-293 cells led to the same modifications. These modifications observed upon either AVP or AVT stimulation during MßCD treatment probably reflect the number of receptors available for each pathway. The difference between CHO and HEK-293 cells with respect to cAMP accumulation after MßCD treatment can most probably be attributed to a different compartmentalization and/or concentration of the transduction partners involved in the response to AVP, as previously reported for the β_2-adrenergic receptor (Huang et al., 2007) or the δ-opioid receptor (Ostrom et al., 2002). In fact, various interpretations can be proposed to explain the results: (i) the V_{1b} receptor could be localized to cholesterol-rich domains, where it could preferentially couple with $G_{q/11}$ and activate the IP pathway upon AVP or AVT binding, and/or to other (non-cholesterol-rich) domains where it could interact with G_s and signal through the cAMP

Molecular Pharmacology Fast Forward. Published on December 1, 2008 as DOI: 10.1124/mol.108.049031
This article has not been copyedited and formatted. The final version may differ from this version.

pathway; (ii) G_s or other proteins of the cAMP signaling cascade could be sequestered to cholesterol-rich domains, and the disruption of these microdomains with MßCD could increase the available concentration of the sequestered proteins, facilitating the competition between the usual G_q coupling of the V_{1b} receptor and the newly available G_s coupling (Pontier et al., 2008).

The presence of V_{1b} receptors has now been demonstrated in various brain regions. Their function has been recently highlighted. Indeed, the only currently available specific antagonist, SSR149415, was shown to exert anxiolytic and antidepressant effects in animal models (Serradeil-Le Gal et al., 2002). However, nothing is known about how the V_{1b} receptor exerts its effects in the brain. The present work increases our understanding of V_{1b} pharmacology by showing that the receptor can activate two different signaling pathways depending on its localization within the plasma membrane. Furthermore, the observation that the relative intensities of agonist effects on the two signaling pathways vary strongly with their molecular structure opens new perspectives to the design of ligands that could be used to selectively activate or inhibit one or the other pathway and thereby specifically modulate particular V_{1b} receptor-regulated functions within the central nervous system.

Acknowledgments

We thank M. Manning and G. Guillon for providing the d[Cha^4]AVP agonist, C. Serradeil-Le Gal (Sanofi-Aventis, Toulouse, France) for the SSR149415 non-peptidic antagonist, and F. Maurin, N. Gregor, and E. Trinquet (Cisbio bioassays, Bagnols-sur-Cèze, France) for the fluorophore-labeled antibodies. The clones of the HA-tagged human $GABA_{B2}$ receptor and the human $5HT_{1a}$ receptor were kindly provided by the group of J.P. Pin and A. Varrault. We also thank the Plateforme de Pharmacologie-Criblage of Montpellier and the Région Languedoc-Roussillon.

References

Abel A, Wittau N, Wieland T, Schultz G and Kalkbrenner F (2000) Cell cycle-dependent coupling of the vasopressin V_{1a} receptor to different G proteins. *J Biol Chem* **275**:32543-32551.

Albizu L, Balestre MN, Breton Ch, Pin JPh, Manning M, Mouillac B, Barberis C and Durroux T (2006) Probing the existence of G protein-coupled receptor dimers by positive and negative ligand-dependent cooperative binding. *Mol Pharmacol* **70**:1783-1791.

Arunlakshana 0 and Schild HO (1959) Some quantitative uses of drug antagonists. *Br J Pharmacol* **14**:48-58.

Ashkenazi A, Winslow JW, Peralta EG, Peterson GL, Schimerlik MI, Capon DJ and Ramachandran J (1987) An M2 muscarinic receptor subtype coupled to both adenylyl cydase and phosphoinositide turnover. *Science* **238**:672-675.

Charest PG, Oligny-Longpré G, Bonin H, Azzi M and Bouvier M (2007) The V_2 vasopressin receptor stimulates ERK1/2 activity independently of heterotrimeric G protein signalling. *Cell Signaling* 19:32-41.

Cussac D, Newman-Tancredi A, Duqueyroix D, Pasteau V and Millan MJ (2002) Differential Activation of $G_{q/11}$ and G_{i3} proteins at 5-Hydroxytryptamine$_{2C}$ receptors revealed by antibody capture assays: influence of receptor reserve and relationship to agonist-directed trafficking. *Mol Pharmacol* **62**:578–589.

Durroux T (2005) Principles: a model for the allosteric interactions between ligand binding sites within a dimeric GPCR. *Trends Pharmacol Sci* **26**:376-384.

Gaillard RC, Schoenenberg P, Favrod-Coune CA, Muller AF, Marie J, Bockaert J and Jard S (1984) Properties of rat anterior pituitary vasopressin receptors: relation to adenylate cyclase and the effect of corticotropin-releasing factor. *Proc. Natl. Acad. Sci. USA* **81**:2907-2911.

Gimpl G and Fahrenholz F (2000) Human oxytocin receptors in cholesterol-rich vs. cholesterol-poor microdomains of the plasma membrane. *Eur J Biochem* **267**:2483-2497.

Gouzènes L, Sabatier N, Richard P, Moos FC and Dayanithi G (1999) V_{1a}- and V_2-type vasopressin receptors mediate vasopressin-induced Ca^{2+} responses in isolated rat supraoptic neurones. *J Physiol* **517**:771-779.

Guillon G, Pena A, Murat B, Derick S, Trueba M, Ventura MA, Szeto HH, Wo N, Stoev S, Cheng LL and Manning M (2006) Position 4 analogues of [deamino-Cys^1] arginine vasopressin exhibit striking species differences for human and rat V_2/V_{1b} receptor selectivity. *J Pept Sci* **12**:190-198.

Guzzi F, Zanchetta D, Cassoni P, Guzzi V, Francolini M, Parenti M and Chini B (2002) Localization of the human oxytocin receptor in caveolin-1 enriched domains turns the receptor-mediated inhibition of cell growth into a proliferative response. *Oncogene* **21**:1658-1667.

Hermans E (2003) Biochemical and pharmacological control of the multiplicity of coupling at G-protein-coupled receptors. *Pharmacol Ther* **99**:25-44.

Hernando F, Schoots O, Lolait SJ and Burbach JPH (2001) Immunohistochemical localization of the vasopressin V_{1b} receptor in the rat brain and pituitary gland: anatomical support for its involvement in the central effects of vasopressin. *Endocrinology* **142**:1659-1668.

Huang P, Xu W, Yoon SI, Chen C, Chong PL and Liu-Chen LY (2007) Cholesterol reduction by methyl-ß-cyclodextrin attenuates the delta opioid receptor-mediated signaling in neuronal cells but enhances it in non-neuronal cells. *Biochem Pharmacol* **73**:534-549.

Hurbin A, Boissin-Agasse L, Orcel H, Rabié A, Joux N, Desarménien MG, Richard Ph and Moos FC (1998) The V_{1a} and V_{1b}, but not V_2, vasopressin receptor genes are expressed in the supraoptic nucleus of the rat hypothalamus, and the transcripts are essentially colocalized in the vasopressinergic magnocellular neurones. *Endocrinology* **139**: 4701-4707.

Jard S, Gaillard RC, Guillon G, Marie J, Schoenenberg P, Muller AF, Manning M and Sawyer WH (1986) Vasopressin antagonists allow demonstration of a novel type of vasopressin receptor in the rat adenohypophysis. *Mol Pharmacol* **30**:171-177.

Kenakin T (2003) Ligand-selective receptor conformations revisited: the promise and the problem. *Trends Pharmacol Sci* **24**:346-354.

Kilsdonk EP, Yancey PG, Stoudt GW, Bangerter FW, Johnson WJ, Phillips MC and Rothblat GH (1995) Cellular cholesterol efflux mediated by cyclodextrins. *J Biol Chem* **270**:17250–17256.

Liu J and Wess J (1996) Different single receptor domains determine the distinct G protein coupling profiles of members of the vasopressin receptor family. *J Biol Chem* **271**:8772-8778.

Lolait SJ, O'Carroll AM, Mahan LC, Felder CC, Button DC, Scott Young III W, Mezey E and Brownstein MJ (1995) Extrapituitary expression of the rat V_{1b} vasopressin receptor gene. *Proc Natl Acad Sci USA* **92**:6783-6787.

Maurel D, Kniazeff J, Mathis G, Trinquet E, Pin JPh and Ansanay H (2004) Cell surface detection of membrane protein interaction with homogeneous time-resolved fluorescence resonance energy transfer technology. *Anal Biochem* **329**:253-262.

Michel MC and Alewijnse AE (2007) Ligand-directed signaling: 50 ways to find a lover. *Mol Pharmacol* **72**:1359-1368.

Milligan G (2006) G-protein-coupled receptor heterodimers: pharmacology, function and relevance to drug discovery. *Drug Discov Today* **11**:541-549.

Miura Y, Hanada K and Jones TL (2001) G_s signaling is intact after disruption of lipid rafts. *Biochemistry* **40**:15418-15423.

Ostrom RS, Liu X, Head BP, Gregorian C, Seasholtz TM and Insel PA (2002) Localization of adenylyl cyclase isoforms and G protein-coupled receptors in vascular smooth muscle cells: expression in caveolin-rich and noncaveolin domains. *Mol Pharmacol* **62**:983-992.

Park PSH and Palczewski K (2005) Diversifying the repertoire of G protein-coupled receptors through oligomerization. *Proc Natl Acad Sci USA* **102**:8793-8794.

Pontier SM, Percherancier Y, Galandrin S, Breit A, Galés C and Bouvier M (2008) Cholesterol-dependent separation of the beta2-adrenergic receptor from its partners determines

signaling efficacy: insight into nanoscale organization of signal transduction. *J Biol Chem* **283**:24659-24672.

Rimoldi V, Reversi A, Taverna E, Rosa P, Francolini M, Cassoni P, Parenti M and Chini B (2003) Oxytocin receptor elicits different EGFR/MAPK activation patterns depending on its localization in caveolin-1 enriched domains. *Oncogene* **22**:6054-6060.

Robert J, Auzan C, Ventura MA and Clauser E (2005) Mechanisms of cell-surface rerouting of an endoplasmic reticulum-retained mutant of the vasopressin V_{1b}/V_3 receptor by a pharmacological chaperone. *J Biol Chem* **280**:42198-42206.

Sabatier N, Richard P and Dayanithi G (1998) Activation of multiple intracellular transduction signals by vasopressin in vasopressin-sensitive neurones of the rat supraoptic nucleus. *J Physiol* **513**:699-710.

Schulte G and Levy FO (2007) Novel aspects of G-protein-coupled receptor signalling - different ways to achieve specificity. *Acta Physiol (Oxf)* **190**:33-38.

Serradeil-Le Gal C, Wagnon J, Simiand J, Griebel G, Lacour C, Guillon G, Barberis C, Brossard G, Soubrié Ph, Nisato D, Pascal M, Pruss R, Scatton B, Maffrand JP and Le Fur G (2002) Characterization of (2*S*,4*R*)-1-[5-chloro-1-[(2,4-dimethoxyphenyl)sulfonyl]-3-(2-methoxy-phenyl)-2-oxo-2,3-dihydro-1*H*-indol-3-yl]-4-hydroxy-*N*,*N*-dimethyl-2-pyrrolidine carboxyamide (SSR149415), a selective and orally active vasopressin V_{1b} receptor antagonist. *J Pharmacol Exp Therap* **300**:1122-1130.

Springael JY, Le Minh PN, Urizar E, Costagliola S, Vassart G and Parmentier M (2006) Allosteric modulation of binding properties between units of chemokine receptor homo- and hetero-oligomers. *Mol Pharmacol* **69**:1652-1661

Strakova Z and Soloff MS (1997) Coupling of oxytocin receptor to G proteins in rat myometrium during labor: Gi receptor interaction. *Am J Physiol* **272**:E870-E876.

Swaminath G, Deupi X, Lee TW, Zhu W, Thian FS, Kobilka TS and Kobilka B (2005) Probing the beta2 adrenoceptor binding site with catechol reveals differences in binding and activation by agonists and partial agonists. *J Biol Chem* **280**:22165-22171.

Terrillon S and Bouvier M (2004) Roles of G-protein-coupled receptor dimerization. *EMBO Rep* **5**:30-34.

Terrillon S, Durroux T, Mouillac B, Breit A, Ayoub MA, Taulan M, Jockers R, Barberis C and Bouvier M (2003) Oxytocin and vasopressin V_{1a} and V_2 receptors form constitutive homo- and heterodimers during biosynthesis. *Mol Endocrinol* **17**:677-691.

Thibonnier M, Preston JA, Dulin N, Wilkins PL, Berti-Mattera LN and Mattera R (1997) The human V_3 pituitary vasopressin receptor: ligand binding profile and density-dependent signaling pathways. *Endocrinology* **138**:4109-4122.

Urban JD, Clarke WP, von Zastrow M, Nichols DE, Kobilka B, Weinstein H, Javitch JA, Roth BL, Christopoulos A, Sexton PM, Miller KJ, Spedding M and Mailman RB (2007) Functional selectivity and classical concepts of quantitative pharmacology. *J Pharmacol Exp Therap* **320**:1–13.

Urizar E, Montanelli L, Loy T, Bonomi M, Swillens S, Gales C, Bouvier M, Smits G, Vassart G and Costagliola S (2005) Glycoprotein hormone receptors: link between receptor homodimerization and negative cooperativity. *EMBO J* **24**:1954-64.

Vaccari C, Lolait SJ and Ostrowski NL (1998) Comparative distribution of vasopressin V_{1b} and oxytocin receptor messenger ribonucleic acids in brain. *Endocrinology* **139**:5015-5033.

Young WS, Li J, Wersinger SR and Palkovits M (2006) The vasopressin 1b receptor is prominent in the hippocampal area CA_2 where it is unaffected by restraint stress or adrenalectomy. *Neuroscience* **143**:1031-1039.

Zhou XB, Lutz S, Steffens F, Korth M and Wieland T (2007) Oxytocin receptors differentially signals via G_q and G_i proteins in pregnant and nonpregnant rat uterine myocytes: implication for myometrial contractility. *Mol Endocrinol* **21**:740-752.

Molecular Pharmacology Fast Forward. Published on December 1, 2008 as DOI: 10.1124/mol.108.049031
This article has not been copyedited and formatted. The final version may differ from this version.

Footnotes

This work was supported by grants from the Centre National de la Recherche Scientifique, the Institut National de la Santé et de la Recherche Médicale, the Universities of Montpellier I and Montpellier II, the European Community (#LSBH-CT-2003-503337), and the Agence Nationale de la Recherche (#ANR-05-NEUR-035-04).

Address correspondence to: Dr Alain Rabié, Institut de Génomique Fonctionnelle, 141 rue de la Cardonille, 34094 MONTPELLIER Cedex 5, France. E-mail: alain.rabie@igf.cnrs.fr

Molecular Pharmacology Fast Forward. Published on December 1, 2008 as DOI: 10.1124/mol.108.049031
This article has not been copyedited and formatted. The final version may differ from this version.

Legends for figures

Fig. 1. Activation of the IP and cAMP pathways in CHO (A), HEK-293 (B), and COS-7 (C) cells. Cells transfected with DNA encoding the rat V_{1b} receptor were stimulated with increasing concentrations of AVP. Accumulation of IP_1 and cAMP were measured in the three cell lines. As negative controls, cells transfected with empty vector (Mock) were also stimulated with AVP. Bars: s.e.m. Statistical analysis : two-way analysis of variance (pathway vs. ligand concentration), pathway: $p<0.001$ for A-C; concentration: $p<0.001$ for A-C; post-hoc Duncan's multiple range test for difference between means: A, $p<0.05$ for log[AVP]=-7, $p<0.01$ for -9.5, $p<0.001$ for -9 to -7.5; B, $p<0.05$ for -7, $p<0.001$ for -9 to -7.5; C, $p<0.01$ for -7 and -9, $p<0.001$ for -8.5 to -7.5).

Fig. 2. Effect of Ctx and Ptx treatment on the AVP-induced cAMP accumulation. CHO cells transfected with DNA encoding the rat V_{1b} receptor were treated (+Ctx, +Ptx) or not (-Ctx, -Ptx) overnight with Ctx (A) or Ptx (B) and then stimulated with increasing concentrations of AVP. Bars: s.e.m.

Fig. 3. Inactivation of IP_1 (A) and cAMP (B) accumulation in V_{1b} receptor transfected CHO cells by SSR149415. CHO cells transfected with rat V_{1b} receptor-encoding DNA were simultaneously stimulated with increasing concentrations of AVP and inhibited by increasing concentrations of SSR149415, a non-peptide specific antagonist of the V_{1b} receptor. Corresponding Arunlakshana-Schild plots of IP_1 and cAMP accumulations (C). Bars: s.e.m.

Fig. 4. IP_1 and cAMP accumulation in CHO cells transfected with rat V_{1b} receptor-encoding DNA and activated by increasing concentrations of two analogs of AVP, AVT (A) and d[Cha^4]AVP (B). Bars: s.e.m. Statistical analysis : two-way analysis of variance (pathway vs. ligand concentration), A, pathway: $p<0.001$; concentration: $p<0.001$; post-hoc Duncan's multiple range test for difference between means: A, $p<0.01$ for log[AVP]=-8, $p<0.001$ for -9.5 to -8.5; B, not significant).

Molecular Pharmacology Fast Forward. Published on December 1, 2008 as DOI: 10.1124/mol.108.049031
This article has not been copyedited and formatted. The final version may differ from this version.

Fig. 5. Detection of dimers of V_{1b} receptors at the plasma membrane of transiently transfected COS-7 cells. A, FRET signal obtained with 6xHis-tagged V_{1a} and V_{1b} receptors. Mock: cells transfected with the carrier plasmid only. Cells transfected with 6xHis-tagged V_{1b} receptor-encoding DNA were incubated or not with V_{1b}-specific (SSR149415) antagonist (1 µM, overnight). B, Corresponding 6xHis-ELISA signal in the cells transfected with 6xHis-V_{1b} receptor-encoding DNA. C, Negative control for dimerization. FRET signal between HA- and 6xHis-tagged V_{1b} receptors, and between HA-$GABA_{B2}$ (GB_2) receptor and 6xHis-V_{1b} receptor, after co-transfection in COS-7 cells treated or not with the V_{1b}-specific antagonist (SSR149415). D, Corresponding HA-ELISA signal. In spite of an essentially equivalent ELISA signal at the plasma membrane, the GB_2 receptor only gave a very low FRET signal with the V_{1b} receptor compared to the V_{1b}/V_{1b} signal. Bars: s.e.m. Statistical analysis : A and B, one-way analysis of variance, $p<0.001$ for A and B; post-hoc Duncan's multiple range test for difference between means: ** $p<0.01$, *** $p<0.001$, difference from 6xHis-V_{1b}; C and D, two-way analysis of variance (transfection vs. SSR149415), $p<0.01$ for C, not significant for D; post-hoc Duncan's multiple range test for difference between means: C, effect of SSR149415, *** $p<0.001$.

Fig. 6. Effect of lowering plasma membrane cholesterol by MßCD in HEK-293 cells. HEK-293 cells transfected with V_{1b} receptor-encoding DNA were treated (+MßCD) or not (-MßCD) with MßCD and stimulated with increasing concentrations of AVP, AVT or d[Cha^4]AVP. Effect on IP_1 (A,C,E) and cAMP (B,D,F) accumulation in cells stimulated with AVP, AVT and d[Cha^4]AVP, respectively. G, Effect of MßCD on cAMP accumulation in wild-type HEK-293 cells incubated with 50 µM forskolin. Bars: s.e.m. Statistical analysis : two-way analysis of variance (pathway vs. agonist concentration) for A-F, pathway: $p<0.001$ for A-F; concentration: $p<0.001$ for A-F; post-hoc Duncan's multiple range test for difference between means: A, $p<0.05$ for -9 and -8.5, $p<0.001$ for -8 to -6; B, $p<0.001$ for -8.5 to -6; C, $p<0.01$ for -8.5, $p<0.001$ for -8 to -6; D, $p<0.001$ for -8.5 to -6; E, $p<0.01$ for -7, $p<0.001$ for -6.5 and -6; F, $p<0.05$ for -9, $p<0.01$ for -8, $p<0.001$ for -7.5 to -6; two-way analysis of variance for G (MßCD vs. forskolin), not significant.

Molecular Pharmacology Fast Forward. Published on December 1, 2008 as DOI: 10.1124/mol.108.049031
This article has not been copyedited and formatted. The final version may differ from this version.

Tables

TABLE 1

Pharmacological properties of CHO, HEK-293, and COS-7 cells transfected with rat vasopressin V_{1b} receptor-encoding DNA.

Affinities, B_{max} for AVP, number of receptors/cell, characteristics (EC_{50}, Hill coefficient) of the responses to AVP stimulation are reported. nd: not determined because of the expression of endogenous V_2 receptor. Mean ± s.e.m.

	CHO-V_{1b}	**HEK-293-V_{1b}**	**COS-7-V_{1b}**
Binding [^{3}H]AVP			
K_d (AVP) (nM)	5.10 ± 0.68	3.71 ± 0.70	nd
B_{max} (AVP) (pmoles/mg protein)	3.58 ± 0.09	16.7 ± 2.3	nd
V_{1b} receptors/cell (x10^{-3})	448 ± 27	796 ± 171	nd
EC_{50} (nM)			
IP_1 accumulation	6.98 ± 0.77	7.28 ± 0.75	3.84 ± 0.54
cAMP accumulation	22.2 ± 1.6	32.7 ± 2.4	18.6 ± 3.9
Hill coefficient			
IP_1 accumulation	0.78 ± 0.07	0.80 ± 0.06	1.11 ± 0.15
cAMP accumulation	1.07 ± 0.07	1.42 ± 0.13	0.78 ± 0.12
Maximal value (pmoles/well)			
IP_1 accumulation	29.2 ± 0.6	23.6 ± 0.5	77.8 ± 1.6
cAMP accumulation	1.56 ± 0.03	0.36 ± 0.02	6.41 ± 0.12

Molecular Pharmacology Fast Forward. Published on December 1, 2008 as DOI: 10.1124/mol.108.049031
This article has not been copyedited and formatted. The final version may differ from this version.

TABLE 2

Characteristics of the response curves to different antagonist or agonists in CHO cells transfected with rat V_{1b} receptor-encoding DNA.

#, K_i for SSR149415 was reported by Serradeil-Le Gal et al. (2002); ##, K_d for d[Cha^4]AVP was described by Guillon et al. (2006). The K_{inact} of SSR149415 were derived from the pA2 of the Arunlakshana-Schild plots (Fig. 3). Mean ± s.e.m. Student *t* test: agonists, difference with AVP, *, $p<0.05$, **, $p<0.01$, ***, $p<0.001$.

	SSR149415	**AVP**	**AVT**	**d[Cha^4]AVP**
Binding [^{3}H]AVP				
K_i or K_d (nM)	1.3 #	5.10 ± 0.68	1.79 ± 0.20***	1.4 ##
K_{inact} or EC_{50} (nM)				
IP_1 accumulation	0.72	6.98 ± 0.77	2.48 ± 0.33**	49.6 ± 8.1**
cAMP accumulation	0.10	22.2 ± 1.6	7.22 ± 0.37***	32.7 ± 6.1
Hill coefficient				
IP_1 accumulation	-	0.78 ± 0.07	0.75 ± 0.07	1.16 ± 0.18
cAMP accumulation	-	1.07 ± 0.07	1.67 ± 0.14*	1.05 ± 0.15
Maximal value (pmoles/well)				
IP_1 accumulation	-	29.2 ± 0.6	30.3 ± 0.6	23.8 ± 1.0**
cAMP accumulation	-	1.56 ± 0.03	2.13 ± 0.03***	0.64 ± 0.03***

Molecular Pharmacology Fast Forward. Published on December 1, 2008 as DOI: 10.1124/mol.108.049031
This article has not been copyedited and formatted. The final version may differ from this version.

TABLE 3

Characteristics of the response curves to AVP, AVT and d[Cha^4]AVP in HEK-293 cells transfected with rat V_{1b} receptor-encoding DNA. The cells were treated (+MßCD) or not (-MßCD) with MßCD. Mean ± s.e.m. Student *t* test: MßCD effect, **, $p<0.01$, ***, $p<0.001$.

Ligand	**AVP**		**AVT**		**d[Cha^4]AVP**	
	-MßCD	+MßCD	-MßCD	+MßCD	-MßCD	+MßCD
EC_{50} (nM)						
IP_1 accumulation	7.3 ± 0.8	5.5 ± 0.7	4.9 ± 0.4	4.2 ± 0.4	107 ± 14	100 ± 21
cAMP accumulation	32.7 ± 2.4	13.1 ± 0.8**	16.3 ± 1.3	6.8 ± 0.5**	103 ± 12	106 ± 72
Hill coefficient						
IP_1 accumulation	0.80 ± 0.06	1.08 ± 0.13	1.08 ± 0.09	1.03 ± 0.08	1.21 ± 0.15	0.77 ± 0.08
cAMP accumulation	1.42 ± 0.13	1.32 ± 0.1	1.60 ± 0.18	1.84 ± 0.21	0.74 ± 0.41	0.58 ± 0.16
Maximal value (pmoles/well)						
IP_1 accumulation	69.1 ± 1.5	47.0 ± 1.1***	66.2 ± 1.1	45.7 ± 0.7***	54.9 ± 2.5	57.7 ± 18.7
cAMP accumulation	0.55 ± 0.01	1.83 ± 0.03***	0.35 ± 0.01	1.26 ± 0.02***	0.09 ± 0.01	0.49 ± 0.08***

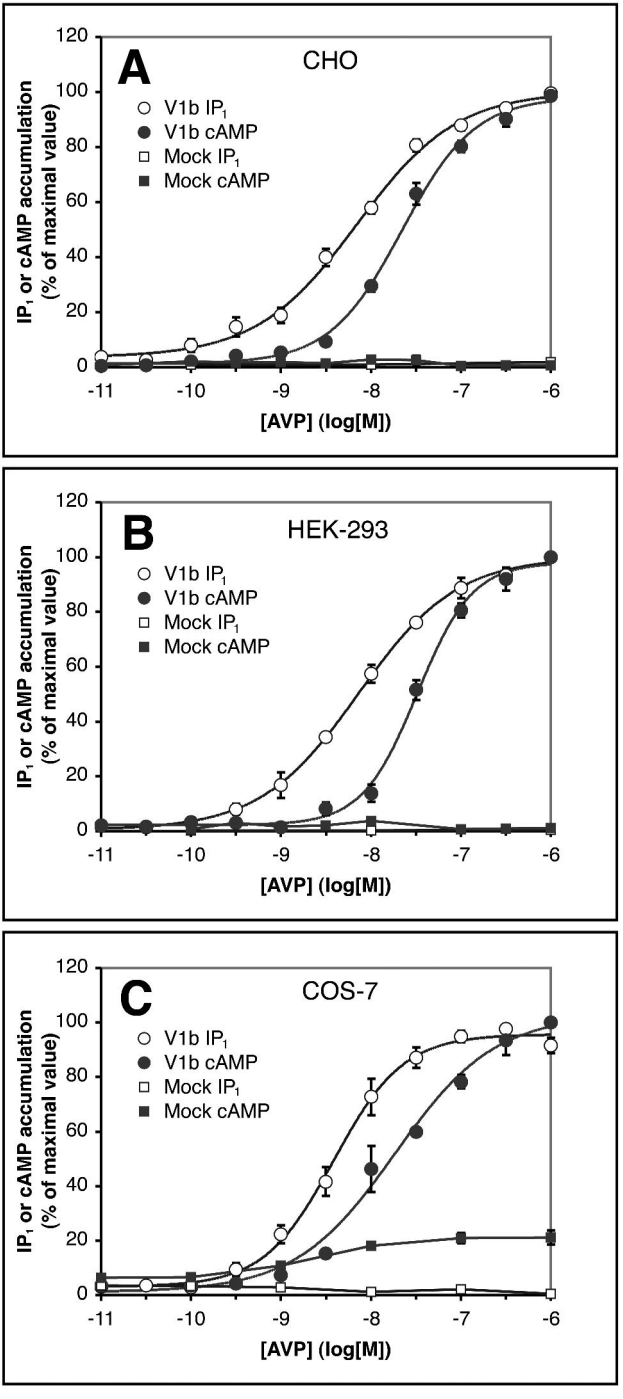
A
CHO
V1b IP1
V1b cAMP
Mock IP1
Mock cAMP
IP1 or cAMP accumulation (% of maximal value)
[AVP] (log[M])
B
HEK-293
C
COS-7

Figure 1

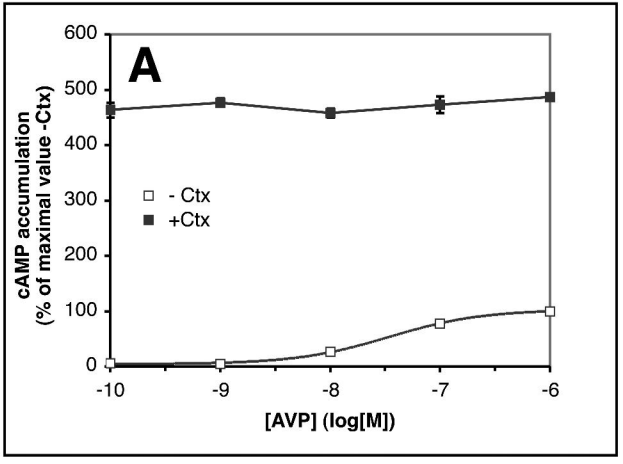
A
cAMP accumulation
(% of maximal value -Ctx)
600
500
400
300
200
100
0
- Ctx
+Ctx
-10
-9
-8
-7
-6
[AVP] (log[M])

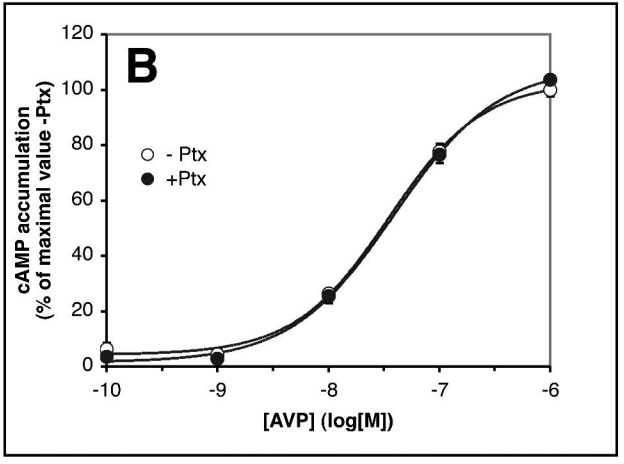
B
cAMP accumulation
(% of maximal value -Ptx)
120
100
80
60
40
20
0
- Ptx
+Ptx
-10
-9
-8
-7
-6
[AVP] (log[M])

Figure 2

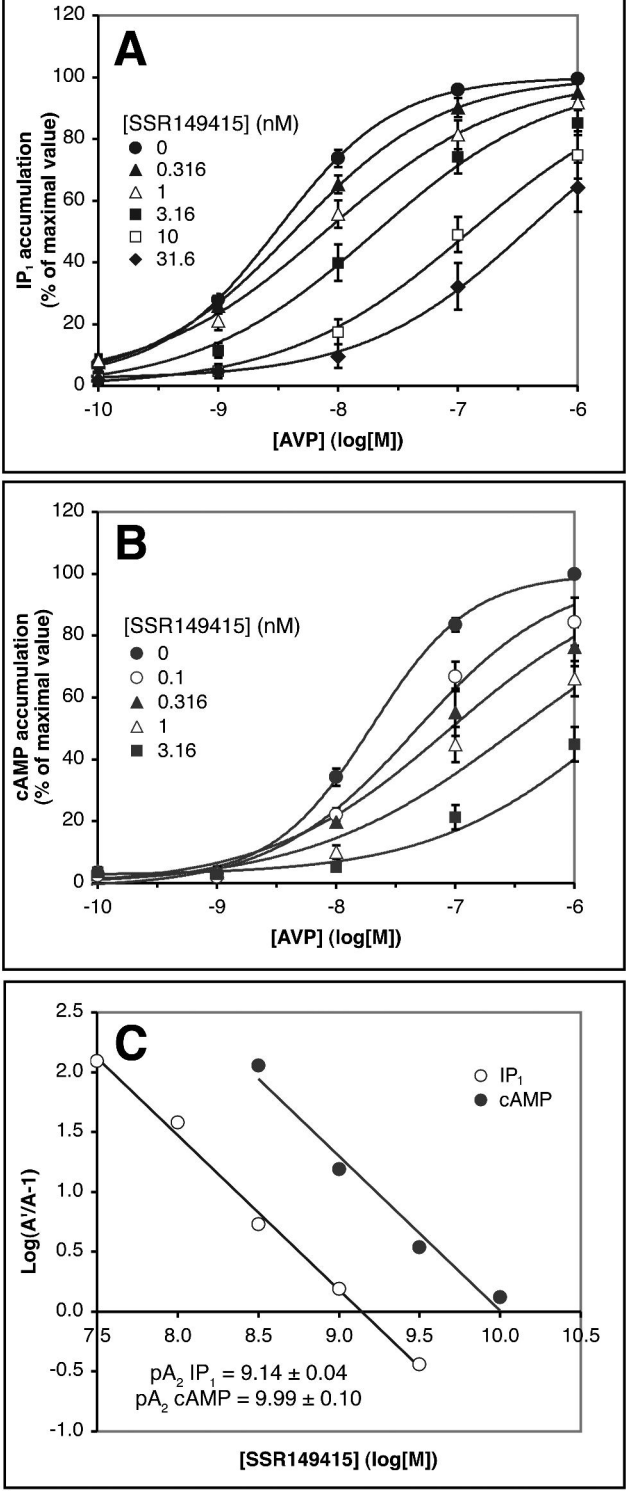
A
IP1 accumulation (% of maximal value)
[SSR149415] (nM)
0
0.316
1
3.16
10
31.6
[AVP] (log[M])
B
cAMP accumulation (% of maximal value)
[SSR149415] (nM)
0
0.1
0.316
1
3.16
[AVP] (log[M])
C
IP1
cAMP
Log(A'/A-1)
pA2 IP1 = 9.14 ± 0.04
pA2 cAMP = 9.99 ± 0.10
[SSR149415] (log[M])

Figure 3

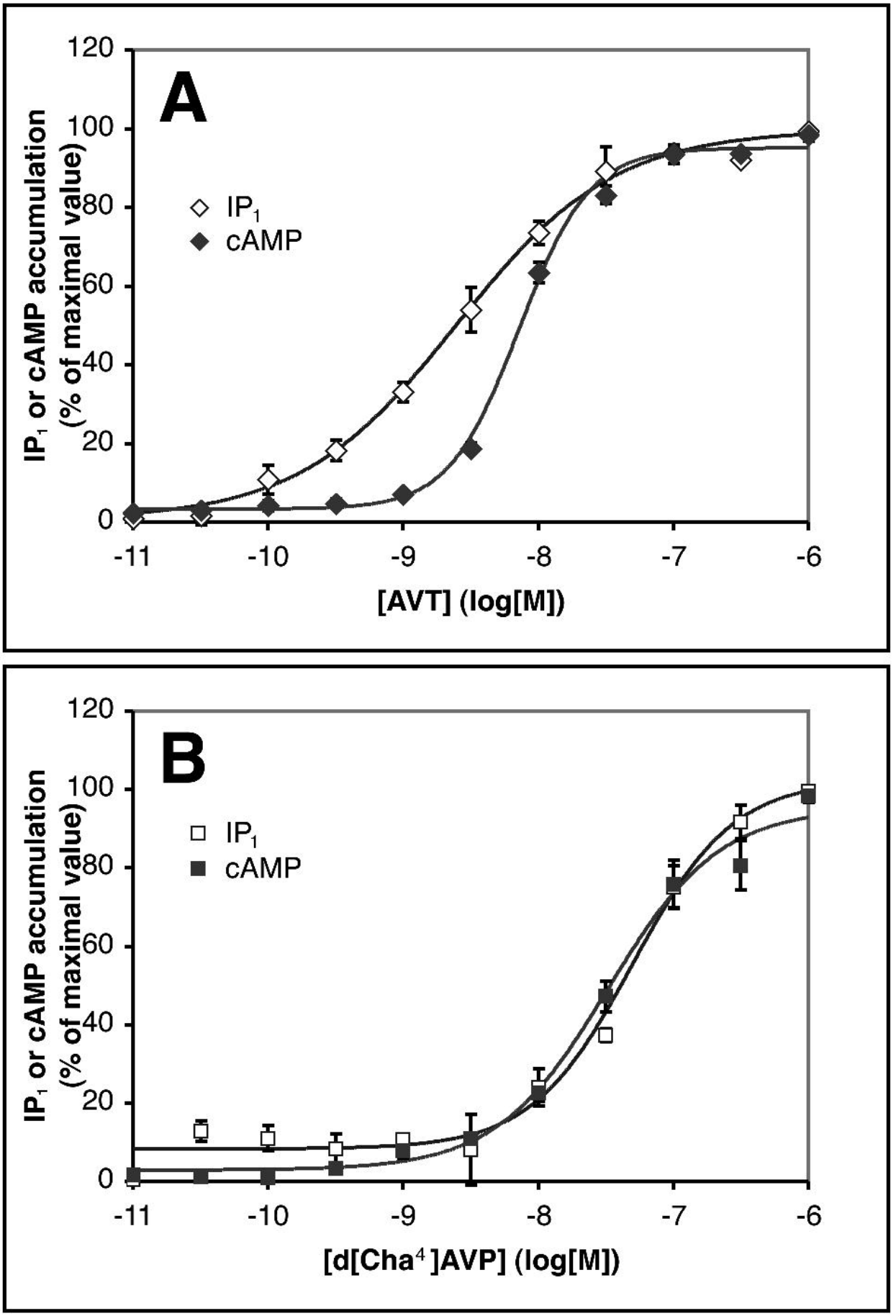
A
IP1
cAMP
IP1 or cAMP accumulation (% of maximal value)
120
100
80
60
40
20
0
-11
-10
-9
-8
-7
-6
[AVT] (log[M])
B
IP1
cAMP
IP1 or cAMP accumulation (% of maximal value)
120
100
80
60
40
20
0
-11
-10
-9
-8
-7
-6
[d[Cha4]AVP] (log[M])

Figure 4

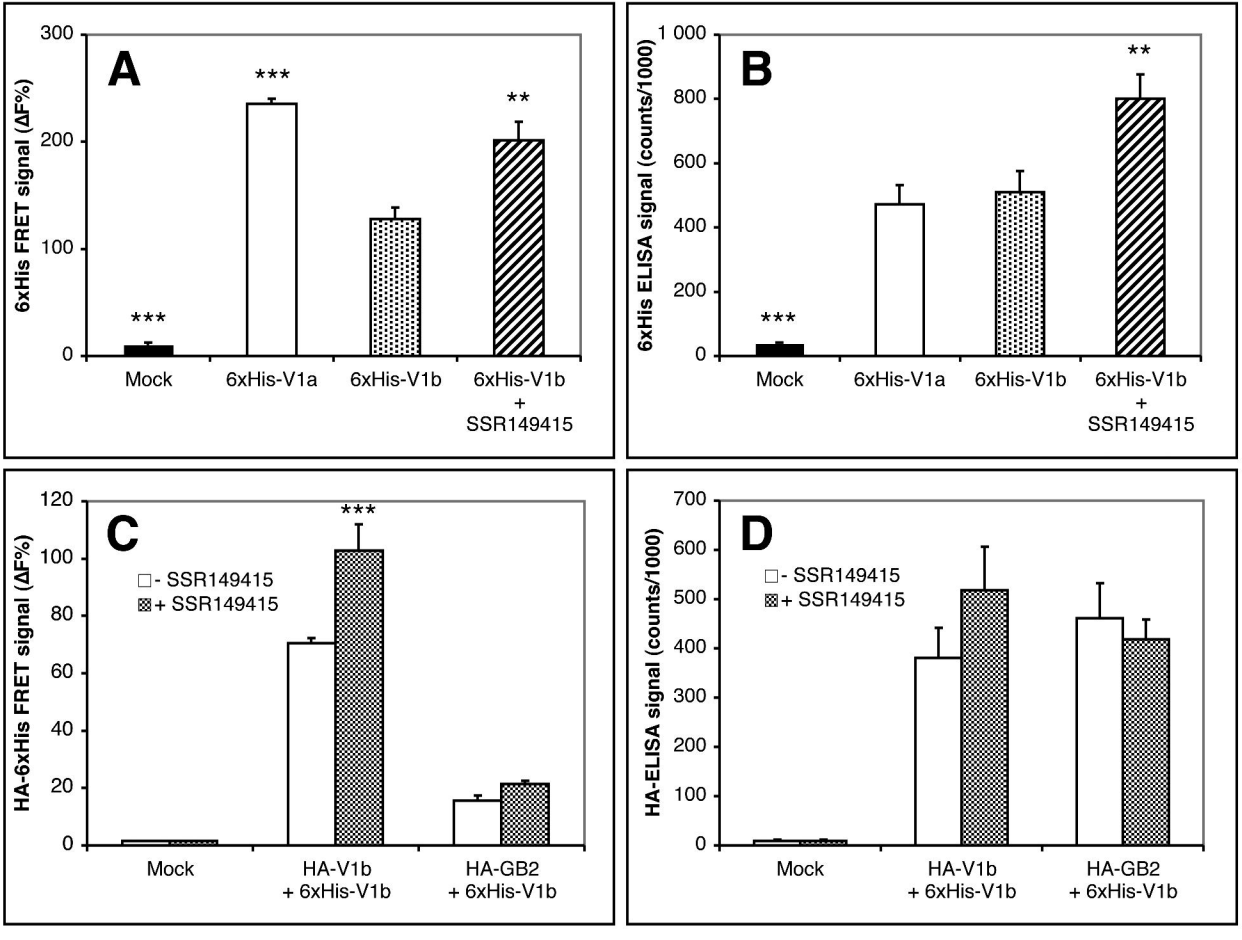
A
6xHis FRET signal (ΔF%)
300
200
100
0
***
***
**
Mock
6xHis-V1a
6xHis-V1b
6xHis-V1b + SSR149415
B
6xHis ELISA signal (counts/1000)
1 000
800
600
400
200
0
***
**
Mock
6xHis-V1a
6xHis-V1b
6xHis-V1b + SSR149415
C
HA-6xHis FRET signal (ΔF%)
120
100
80
60
40
20
0
***
□- SSR149415
▨+ SSR149415
Mock
HA-V1b + 6xHis-V1b
HA-GB2 + 6xHis-V1b
D
HA-ELISA signal (counts/1000)
700
600
500
400
300
200
100
0
□- SSR149415
▨+ SSR149415
Mock
HA-V1b + 6xHis-V1b
HA-GB2 + 6xHis-V1b

Figure 5

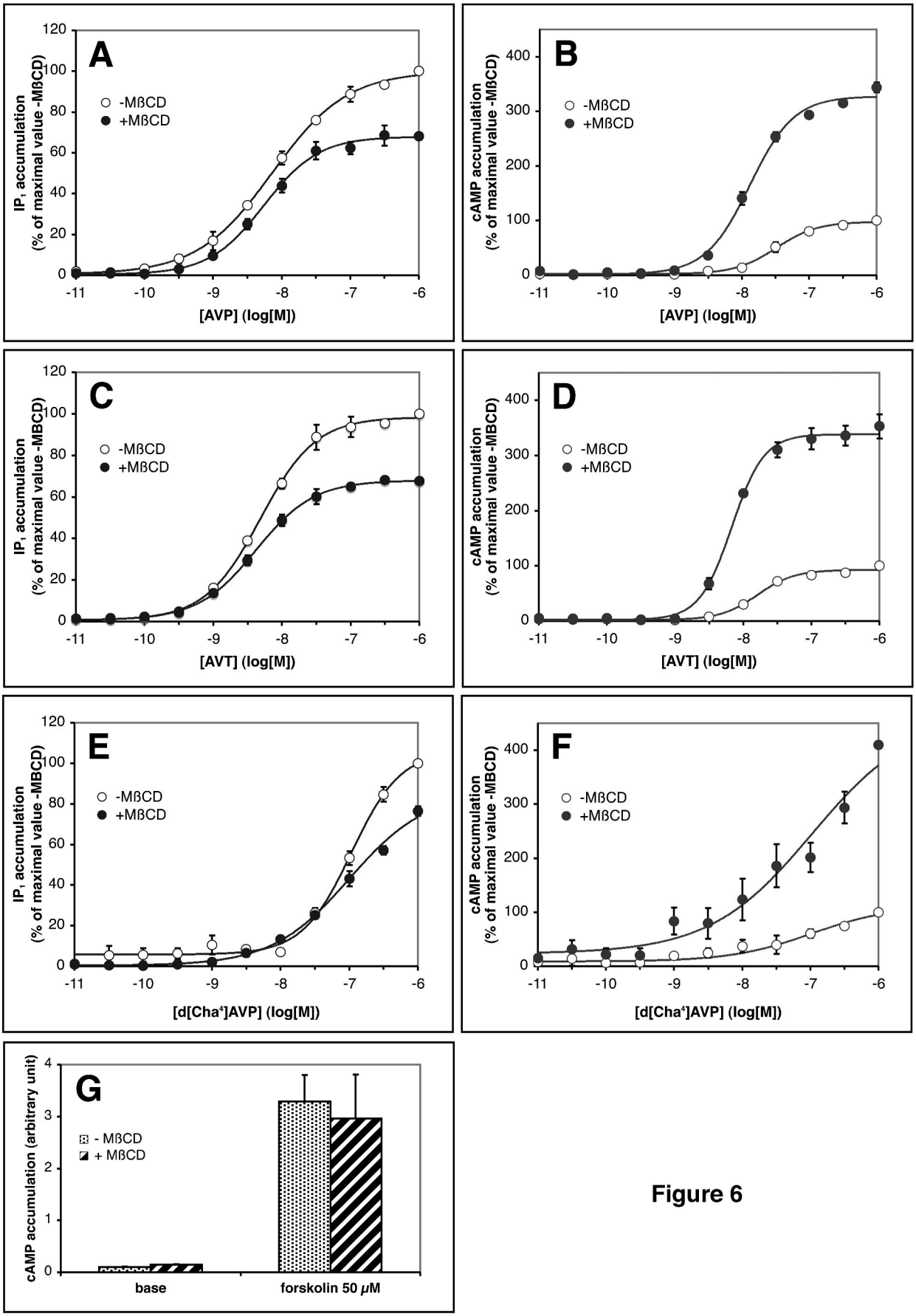
A
-MßCD
+MßCD
IP1 accumulation (% of maximal value -MßCD)
[AVP] (log[M])
B
-MßCD
+MßCD
cAMP accumulation (% of maximal value -MßCD)
[AVP] (log[M])
C
-MßCD
+MßCD
IP1 accumulation (% of maximal value -MBCD)
[AVT] (log[M])
D
-MßCD
+MßCD
cAMP accumulation (% of maximal value -MBCD)
[AVT] (log[M])
E
-MßCD
+MßCD
IP1 accumulation (% of maximal value -MBCD)
[d[Cha4]AVP] (log[M])
F
-MßCD
+MßCD
cAMP accumulation (% of maximal value -MBCD)
[d[Cha4]AVP] (log[M])
G
- MßCD
+ MßCD
cAMP accumulation (arbitrary unit)
base
forskolin 50 µM

Figure 6